Macroscopic and Microscopic Investigation of Ni(II) Sequestration on Diatomite by Batch, XPS, and EXAFS Techniques

ARTICLE *in* ENVIRONMENTAL SCIENCE & TECHNOLOGY · AUGUST 2011

Impact Factor: 5.33 · DOI: 10.1021/es202108q · Source: PubMed

6 AUTHORS, INCLUDING:

Shitong Yang
Soochow University (PRC)
48 PUBLICATIONS **1,604** CITATIONS
SEE PROFILE

Jiang Sheng
Chinese Academy of Sciences
22 PUBLICATIONS **457** CITATIONS
SEE PROFILE

Xiaoli Tan
Chinese Academy of Sciences
77 PUBLICATIONS **3,581** CITATIONS
SEE PROFILE

Xiangke Wang
Chinese Academy of Sciences
307 PUBLICATIONS **13,375** CITATIONS
SEE PROFILE

Environmental Science & Technology

ARTICLE

pubs.acs.org/est

Macroscopic and Microscopic Investigation of Ni(II) Sequestration on Diatomite by Batch, XPS, and EXAFS Techniques

Guodong Sheng, Shitong Yang, Jiang Sheng, Jun Hu, Xiaoli Tan, and Xiangke Wang*

Key Laboratory of Novel Thin Film Solar Cells, Institute of Plasma Physics, Chinese Academy of Sciences, P.O. Box 1126, Hefei, 230031, P.R. China

Supporting Information

ABSTRACT: Sequestration of Ni(II) on diatomite as a function of time, pH, and temperature was investigated by batch, XPS, and EXAFS techniques. The ionic strength-dependent sorption at pH < 7.0 was consistent with outer-sphere surface complexation, while the ionic strength-independent sorption at pH = 7.0−8.6 was indicative of inner-sphere surface complexation. EXAFS results indicated that the adsorbed Ni(II) consisted of ~6 O at $R_{Ni-O} \approx 2.05$ Å. EXAFS analysis from the second shell suggested that three phenomena occurred at the diatomite/water interface: (1) outer-sphere and/or inner-sphere complexation; (2) dissolution of Si which is the rate limiting step during Ni uptake; and (3) extensive growth of surface (co)precipitates. Under acidic conditions, outer-sphere complexation is the main mechanism controlling Ni uptake, which is in good agreement with the macroscopic results. At contact time of 1 h or 1 day or pH = 7.0−8.0, surface coprecipitates occur concurrently with inner-sphere complexes on diatomite surface, whereas at contact time of 1 month or pH = 10.0, surface (co)precipitates dominate Ni uptake. Furthermore, surface loading increases with temperature increasing, and surface coprecipitates become the dominant mechanism at elevated temperature. The results are important to understand Ni interaction with minerals at the solid−water interface, which is helpful to evaluate the mobility of Ni(II) in the natural environment.

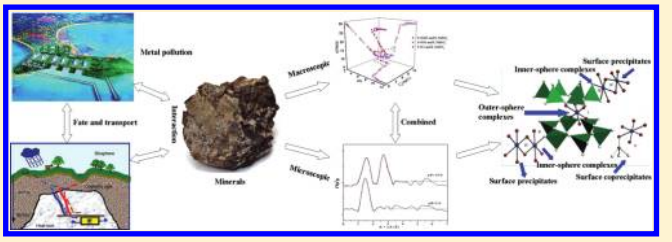

INTRODUCTION

Contamination of the surface and subsurface environment by metals is of worldwide concern,[1] as the fate and mobility of metals are significantly affected by sequestration on minerals that are ubiquitous in soil and sedimentary environments.[1−3] Therefore, a thorough understanding of metal interaction with minerals is of fundamental importance.[2,3] Diatomite is fine-grained, low-density biogenic sediment, which consists of amorphous silica ($SiO_2 \cdot nH_2O$) derived from opalescent frustules of diatoms.[4−6] Due to its high sorption ability and surface area, diatomite can strongly interact with metals, which is important for the evaluation of both the potential environmental application of diatomite and the physicochemical behavior of metals in the natural environment.[4−9] Thus, macroscopic studies have been performed to investigate the effect of environmental conditions on metal sorption on diatomite.[4−9] However, to our knowledge, no attention has been paid to the mechanism of metal sorption onto diatomite at the molecular level. To gain understanding of the sorption mechanism, it is necessary to combine macroscopic and microscopic experiments.[10] A useful spectroscopic technique that can provide important insights into sorption mechanism is the EXAFS technique, which is useful in distinguishing sorption mechanisms such as outer-sphere or inner-sphere surface complexation,[11−13] surface (co)precipitation,[14−18] and oxidation−reduction reaction.[19,20]

Ni(II) is an important contaminant generated in industrial processes such as electricity production in nuclear power plants, and Ni(II) sorption is essential to evaluate its behavior in the environment.[21] In previous studies, a series of experiments[14−18,22−28] have been conducted to investigate Ni(II) uptake on various minerals under neutral to weak alkaline conditions, and it has been found that in the case where the sorbents contained Al including pyrophyllite, gibbsite, and illite, Ni coprecipitated with Al to form a Ni−Al layered double hydroxide (LDH),[14−17,22−26] while in the case of Al-free sorbents such as talc and amorphous silica, Ni(II) formed Ni phyllosilicate coprecipitates.[18,27,28] A dissolution-surface (co)precipitation mechanism was proposed for Ni(II) sorption on alumina[25,26] and on silica and silicates.[28] However, according to our literature survey, all of these studies were limited over a narrow pH range (i.e., pH 7.0−8.5);[14−18,22−28] no study was carried out to investigate the sorption over a wide pH range especially under acidic conditions. More importantly, most of these studies were conducted at high Ni concentration;[14−18,22−28] little attention has been paid to Ni(II) uptake at low concentration that is more representative of the natural environment.[10,29] Strathmann et al.[10] and Dähn et al.[29] studied Ni(II) sorption on boehmite and montmorillonite at low concentration, respectively, and they reported that inner-sphere

Received: June 21, 2011
Accepted: August 19, 2011
Revised: August 18, 2011
Published: August 19, 2011

complexation was the main mechanism controlling Ni(II) uptake. The limited information available on Ni(II) uptake mechanism onto minerals at low concentration, however, limits our ability to adequately assess their actual fate in natural environment.

In addition, temperature in various environmental compartments can fluctuate diurnally, seasonally, and spatially, which can affect the sorption behavior and mechanism, and thus the fate and transport of metals in natural environment.[30] Therefore, mechanistic and quantitative studies of temperature effect on metal sorption can facilitate more accurate prediction of the fate and transport of metals.[30] However, few studies with respect to the effect of temperature on metal sorption by spectroscopic techniques are available.[30,31]

Herein, batch, XPS, and EXAFS techniques were combined to investigate Ni(II) interaction at the diatomite−water interface. As previous works[14−18,22−28] on Ni(II) sorption were conducted at high concentration, this work was carried out at low concentration. The main objective of this study was to characterize the local atomic structures of Ni(II) adsorbed on diatomite over a wide range of pH, time, and temperature and to discriminate the different mechanisms of Ni(II) sorption on minerals at low concentration from those at high concentration.

EXPERIMENTAL SECTION

Materials and Chemicals. All chemicals were purchased in analytical purity and used without further purification. Milli-Q water was used. The diatomite was derived from Shengzhou county (Zhejiang, China) and was milled through a 200-mesh prior to use in the experiments. The detailed chemical components of the diatomite were determined by X-ray fluorescence analysis and the predominant chemical components were SiO_2 (89.6%), Al_2O_3 (2.5%), Fe_2O_3 (1.8%), Na_2O (1.5%), and CaO (0.1%). A comparison for specific chemical components and surface area of diatomite originating from different sources is shown in Table SI-1 in the Supporting Information (SI). The acid−base surface chemistry and binding site of the diatomite was investigated by potentiometric method and the results are shown in the SI.

Batch Experiments. The sorption of Ni(II) on diatomite was investigated by using batch technique in 10-mL polyethylene centrifuge tubes under N_2 conditions. The diatomite suspension and $NaNO_3$ solution were pre-equilibrated for 24 h and then Ni(II) solution was added to achieve desired concentrations of different components. The pH was adjusted to desired value by adding negligible volumes of 0.01 or 0.1 M HNO_3 or NaOH. After the suspensions were shaken for equilibrium, the solid and liquid phases were separated by centrifugation at 9000 rpm for 30 min, which was enough to obtain the clear liquid phase. Radiotracer ^{63}Ni(II) was used in the experiments; the concentration of Ni(II) was analyzed by liquid scintillation counting using a Packard 3100 TR/AB liquid scintillation analyzer (PerkinElmer). The scintillation cocktail was Ultima Gold AB (Packard).

Released Si was measured using a graphite-furnace atomic absorption spectrometer (GF-AAS; Shimadzu, AA-6650) equipped with an autosample exchanger. The pH-dependence and time-dependence of Si released fraction were monitored over 3−12 and 1−300 h, respectively. All of the sample solutions were filtered through a 0.45-μm membrane filter and acidified by 1% HNO_3 before GF-AAS measurements. The detection limit of our system was ∼0.1 ppb.

XPS and EXAFS Study. Sorption samples for XPS and EXAFS analysis were prepared in a manner similar to that described for the batch experiments. Briefly, sorption samples for XPS and EXAFS analysis were conducted using a 1-L vessel with 0.5 g/L diatomite, 0.01 M $NaNO_3$, and 10 mg/L Ni(II) under various conditions.

XPS spectra were recorded on powders with a thermo ESCALAB 250 spectrometer using an Al Kα monochromatized source and a multidetection analyzer under 10^{-8} Pa residual pressure. Surface charging effects were corrected with C1s peak at 284.6 eV as a reference. A Shirley background correction and Gaussian−Lorentzian fitting were used to transform peak areas to total intensities.

Ni(II) K-edge EXAFS spectra at 8333 eV were recorded at ambient temperature at the National Synchrotron Radiation Laboratory (NSRL, China) in fluorescence (for Ni(II)(aq) and Ni(II) sorption samples) and in transmission (for β-$Ni(OH)_2$ and NiO) modes. Energy calibration, fluorescence deadtime correction, and the EXAFS data analysis were performed with the SixPack interface to the IFEFFIT package. EXAFS data reduction and analyses were performed using the procedures described in the SI.

RESULTS AND DISCUSSION

Kinetic Study. Sequestration of Ni(II) on diatomite (Figure 1A) was initially fast, with ∼60% uptake occurring in the first 2 h. Subsequent uptake continued slowly, and ∼80% was adsorbed after 4 h, and then no obvious uptake was found in the following contact time. These bulk uptake results followed the general behavior of metal uptake onto minerals.[32] Sorption onto reactive sites takes place during the initial rapid uptake, while the subsequent slower uptake could be due to sorption onto less reactive sites, diffusion, or formation of surface (co)precipitates.[32]

EXAFS spectra and the radial structure functions (RSFs) of sorption samples for different times are shown in Figure 2. Complex features are found in the EXAFS spectra (Figure 2A), especially at $k > 5.0$ Å^{-1}, indicating the presence of higher shells of Ni. As time increased, more structured features appeared at higher k range and new features can be seen at k ∼5 and ∼7.5 Å^{-1}. It is clear from the two peaks in EXAFS spectra that the local atomic structures of Ni(II) vary with increasing time.

In the RSFs of all samples (Figure 2B), the peak at ∼1.6 Å is indicative of the first shell and the peak at ∼2.8 Å is indicative of the second shell; the peak at 2−2.4 Å is an artifact that is caused by interference from the first and second shells.[32] The presence of the second shell is due to the second neighbor atoms (Ni/Si) surrounding Ni, which is suggestive of the formation of inner-sphere complexes, surface precipitates or coprecipitates. The intensity of the second peak in the RSFs increases with increasing time. The second peak intensity of the sample over 1 month is larger than that of the sample over 1 day, indicating a greater contribution of Ni/Si backscattering with increasing time.

From Table 1, Ni is coordinated with ∼6 O at $R_{Ni-O} \approx 2.05$ Å in the first shell for all samples. The R values suggest no substantial change in the first shell,[33] The second shell fit can be divided into two groups, one includes Ni−Si1 and Ni−Si2 backscattering and the other includes Ni−Ni and Ni−Si2 backscattering. Quantitative analysis led to the identification of two nearest shells containing 1.2 Si at $R_{Ni-Si1} \approx 3.10$ Å and 3.2 Si at $R_{Ni-Si2} \approx 3.28$ Å for the sample over 1 h and 1.8 Si at $R_{Ni-Si1} \approx$ 3.09 Å and 3.4 Si at $R_{Ni-Si2} \approx 3.28$ Å for the sample over 1 day.

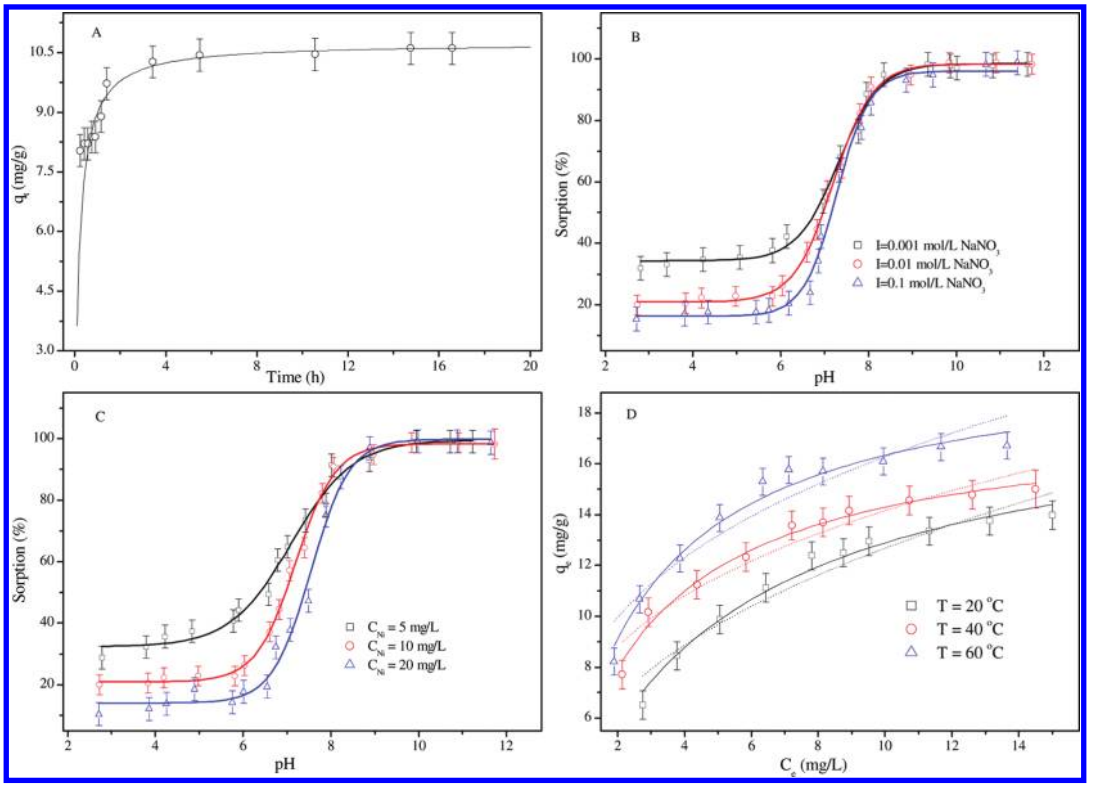

Figure 1. Effect of environmental conditions on Ni(II) sorption to diatomite, m/V = 0.5 g/L. (A) Effect of reaction time, $C_{Ni(II)initial}$ = 10 mg/L, pH = 7.0, T = 20 °C, I = 0.01 M $NaNO_3$. (B) Effect of ionic strength, T = 20 °C, $C_{(Ni)initial}$ = 10 mg/L. (C) Effect of Ni initial concentration, T = 20 °C, I = 0.01 M $NaNO_3$. (D) Sorption isotherms at different temperatures, pH = 7.0, I = 0.01 M $NaNO_3$. Symbols: experimental data; solid lines: Langmuir fitting; dotted lines: Freundlich fitting.

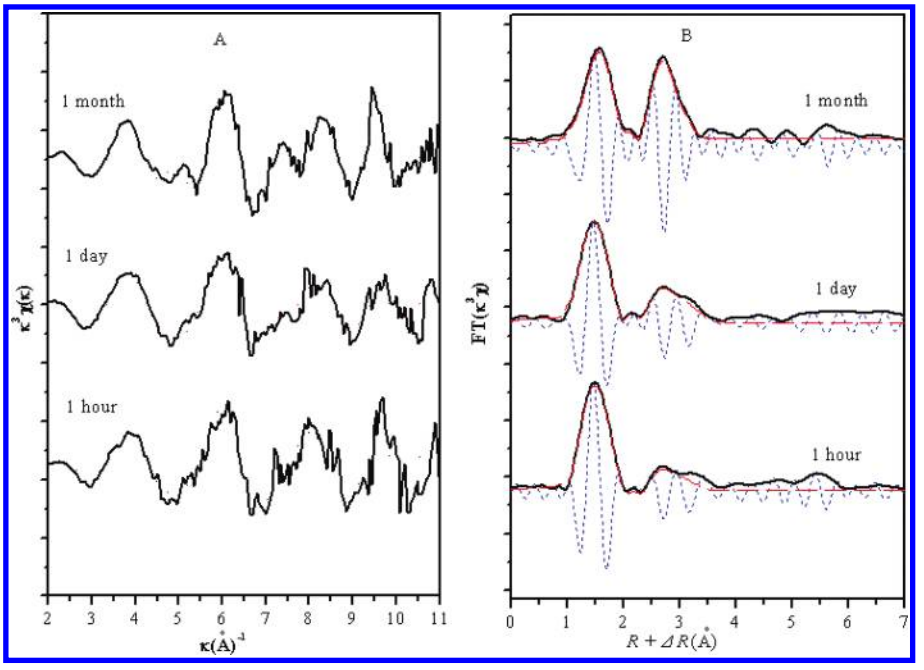

Figure 2. EXAFS spectra (A) and corresponding RSF magnitudes (solid and dashed lines represent experimental spectra and spectral fits, respectively) and imaginary parts (B) of sorption samples at various times; time = 1 h, 1 d, 1 m; $C_{Ni(II)initial}$ = 10 mg/L; pH = 7.0; T = 20 °C; I = 0.01 M $NaNO_3$.

Ni−Ni and Ni−Si2 scattering paths have also been used by EXAFS fitting for the samples (data not shown) and the results are quite similar to those fitted by using Ni−Si1 and Ni−Si2 scattering paths. Due to the similarity of interatomic distances of Ni−Ni and Ni−Si1, they can not be easily distinguished from each other as second-neighbor backscatters, especially in

Table 1. Structural Parameters Derived from EXAFS Analysis for the Reference and Sorption Samples[a]

sample conditions	first shell (Ni−O)			second shell (Ni−Ni/Si)			
	CN	R (Å)	σ^2 (Å^2)	bond	CN	R (Å)	σ^2 (Å^2)
Ni(II)(aq)	6.2	2.06	0.006				
β-Ni(OH)$_2$	6.1	2.04	0.004	Ni−Ni	6.0	3.11	0.007
NiO	6.0	2.05	0.005	Ni−Ni	12.2	2.92	0.007
pH 7.0, 20 °C, 1 h	6.1	2.05	0.005	Ni−Si1(Ni)	1.2	3.10	0.007
				Ni−Si2	3.2	3.28	0.007
pH 7.0, 20 °C, 1 day	6.1	2.05	0.004	Ni−Si1(Ni)	1.8	3.09	0.007
				Ni−Si2	3.4	3.28	0.007
pH 7.0, 20 °C, 1 month	6.1	2.05	0.003	Ni−Ni	3.3	3.07	0.007
				Ni−Si2	3.7	3.27	0.007
pH 5.0, 20 °C, 1 day	6.0	2.04	0.003				
pH 8.0, 20 °C, 1 day	6.0	2.04	0.004	Ni−Si1(Ni)	1.9	3.10	0.007
				Ni−Si2	3.6	3.27	0.007
pH 10.0, 20 °C, 1 day	6.0	2.05	0.003	Ni−Ni	2.9	3.07	0.007
				Ni−Si2	4.4	3.27	0.007
pH 7.0, 40 °C, 1 day	6.1	2.04	0.004	Ni−Si1(Ni)	1.8	3.09	0.007
				Ni−Si2	3.8	3.27	0.007
pH 7.0, 60 °C, 1 day	6.1	2.04	0.005	Ni−Si1(Ni)	1.9	3.09	0.007
				Ni−Si2	4.3	3.27	0.007

[a] R: Interatomic distance; CN: Coordination number; σ^2: Debye-Waller factor; Ni(II)(aq), β-Ni(OH)$_2$, and NiO are named as reference samples, whereas the other samples of diatomite with adsorbed Ni(II) are named as sorption samples.

circumstances where the contribution of both is small and can not be resolved each other in the Fourier transform. Based on these analyses, especially the high coordination numbers of Si atoms at $R_{Ni-Si2} \approx 3.28$ around central Ni (herein, >3), one can conclude that mixed Ni−Si surface coprecipitate (i.e., Ni phyllosilicate) is formed on diatomite surface.[28,34,35] The available Si source was derived from the dissolution of the sorbent during Ni sorption.[28] Charlet and Manceau[28] investigated Ni(II) sorption on silica and silicates using EXAFS technique, and a clay-like-local structure pointed to the coprecipitation of a new hydrous silicate. This neoformation of clays during Ni uptake was thought to occur through the interaction of Ni(II) with dissolved silicic acid, the sorbent acted as a source of silicic acid and eventually as a template. The results of time-dependent Si concentration released in the supernatant of Ni(II)−diatomite systems are given in Figure SI-4A. One can see from Figure SI-4A that a little amount of Si was released at the initial stage. Therefore, the formation of surface coprecipitates somewhat contributes to Ni sorption at the initial stage. However, it should be noted that other sorption processes may occur concurrently with surface coprecipitation as the diatomite samples have Si−OH sites where Ni can potentially be adsorbed as inner surface complexes.

For the sample over 1 month, the best fit of the second shell includes Ni−Ni and Ni−Si2. One can see from Table 1 that the central Ni is surrounded by 3.3 Ni at $R_{Ni-Ni} \approx 3.07$ Å and 3.7 Si at $R_{Ni-Si2} \approx 3.27$ Å, suggesting that mixed Ni−Si surface coprecipitate (i.e., Ni phyllosilicate) is formed.[28,35] Based on the EXAFS results, Schlegel et al.[36] also found that dissolved Si exerted a key role in the nucleation and extensive growth of metal phyllosilicate. One can see from Figure SI-4A that a significant amount of Si was released from diatomite at longer contact time. This phenomenon is ascribed to the fact that metal sorption onto mineral surface can significantly destabilize surface metal ions (e.g., Si) relative to the bulk minerals.[37,38] Combining the Si released results and the EXAFS analysis, one can conclude that Ni(II) phyllosilicate mainly controls Ni uptake on diatomite over extended time. However, it is worth pointing out that Ni surface precipitates can not be excluded due to the similarity of EXAFS spectra in k-space for Ni(OH)$_2$ and Ni phyllosilicate with the sorption samples (Figure SI-5), and thus a mixture of Ni(OH)$_2$ surface precipitates and Ni(II) phyllosilicate formed after reaction time of 1 month. The relative contribution to the overall Ni(II) uptake needs further investigation. Sparks and coworkers[14−18,22] found from extensive kinetic and EXAFS studies that, at high concentration, surface-induced Ni (co)precipitates contributed to the continued uptake of Ni(II) on minerals over the whole time. However, Strathmann et al.[10] studied Ni(II) sorption on boehmite at low concentration, and postulated that the time-invariant nature of EXAFS spectra was attributed to inner-sphere complexation. In contrast to previous studies, we find that, at low Ni concentration, Ni(II) phyllosilicate and inner-sphere complexes simultaneously form on diatomite at initial contact time and Ni surface (co)precipitates dominates Ni uptake at longer contact time.

pH Effect. The sequestration of Ni(II) on diatomite was studied at various solution chemistries and the results are shown in Figure 1B−C. Ni(II) sorption on diatomite is obviously affected by pH. The sorption of Ni(II) increases slowly with pH ranging from 3.0 to 7.0, then increases abruptly at pH 7.0−9.0, and at last maintains high level with increasing pH at pH > 9.0. Approximately 90% of Ni(II) is adsorbed on diatomite at pH > 9.0 (Figure 1B). Figure SI-6A shows the relative distribution of Ni(II) species calculated from the hydrolysis constants listed in Table SI-2. It is clear that Ni(II) presents in the species of Ni^{2+}, $Ni(OH)^+$, $Ni(OH)_2^0$, $Ni(OH)_3^-$, and $Ni(OH)_4^{2-}$ at different pH. At pH < 9.0, the main species is Ni^{2+}.[3] The acid−base titration results (see SI) demonstrate that

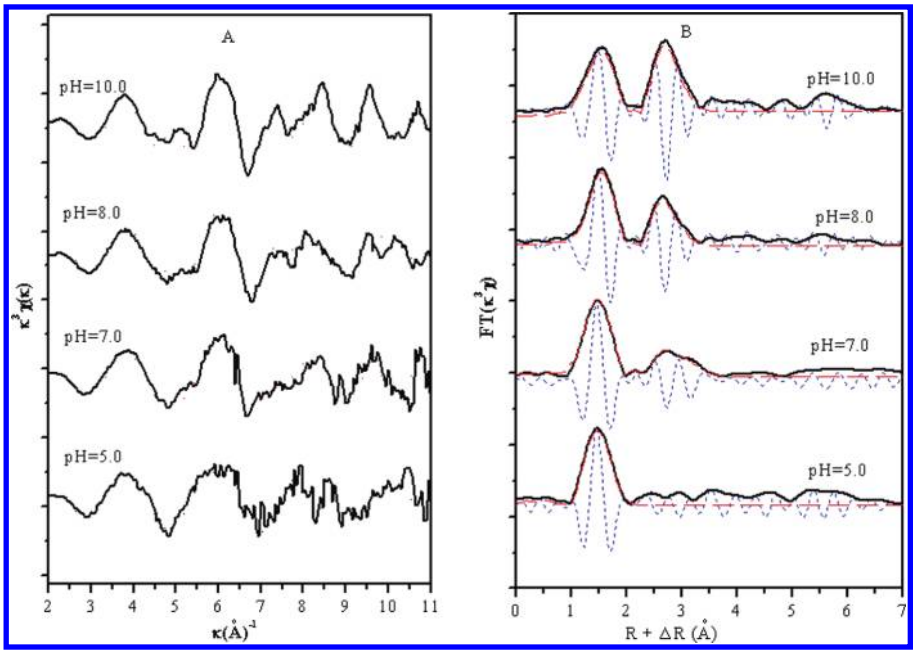

Figure 3. EXAFS spectra (A) and corresponding RSF magnitudes (solid and dashed lines represent experimental spectra and spectral fits, respectively) and imaginary parts (B) of sorption samples at various pH values, $C_{Ni(II)initial}$ = 10 mg/L, pH = 5.0, 7.0, 8.0, 10.0, T = 20 °C, I = 0.01 M $NaNO_3$.

diatomite has two binding sites, ion exchange site (XNa/H) and surface complexation site (XOH), and thus the low Ni(II) uptake under acidic conditions (i.e., pH < 7.0) may be attributed to the competition between H^+/Na^+ and Ni^{2+} with ion exchange site, whereas the abrupt increase of Ni(II) uptake under weak alkaline conditions (i.e., pH 7.0−9.0) may be contributed to Ni^{2+} complexation with surface site (XOH). From the precipitation curve (Figure SI-6B), it can be seen that Ni(II) begins to form precipitation at pH = 8.6 if no Ni(II) is adsorbed on diatomite. Therefore, one can conclude that surface precipitate can contribute to Ni(II) uptake under high alkaline conditions (i.e., pH > 8.6). Figure 1B also shows the ionic strength effect on Ni(II) sorption and the sorption curve can be divided into two pH regions: at pH < 7.0, Ni(II) sorption increases with decreasing ionic strength, while the uptake of Ni(II) is not affected by ionic strength at pH > 7.0. Hayes and Leckie[39] suggested that outer-sphere and inner-sphere complexation could be distinguished by studying ionic strength effect on metal uptake behavior. Outer-sphere complexation is obviously influenced by ionic strength, whereas inner-sphere complexation is not. Herein, the ionic strength-dependent sorption at pH < 7.0 is mainly attributed to outer-sphere complexation, whereas the ionic strength-independent sorption at pH = 7.0−8.6 is mainly dominated by inner-sphere complexation. However, surface precipitate can form at pH > 8.6, and can not be differentiated by the ionic strength effect, which needs to be identified by EXAFS investigation in the next section. Pathak and Choppin[40] investigated Ni(II) sorption on hydrous silica over a narrow pH range of 6.5 to 8.5, and a gradual decrease of sorption with increasing ionic strength in this pH range suggested outer-sphere complexation. In contrast, Saek and Kunito[41] studied Ni(II) sorption on silica as a function of solution pH and observed that Ni(II) sorption increased rapidly from 0 to 100% at a narrow pH range of approximately 2 pH units (i.e., Ni(II) sorption started at pH ∼6.9, and achieved ∼100% at pH ∼8.8). Using a constant capacitance model, they also found Ni(II) formed inner-sphere complexes on silica. Herein, under similar pH conditions, the results of Ni(II) sorption on diatomite are in good agreement with those of Ni(II) sorption on silica,[41] but contradictory with those of Ni(II) sorption on hydrous silica.[40]

Figure 1C shows Ni(II) uptake on diatomite as a function of pH for different Ni(II) initial concentrations. Ni(II) sorption was affected by initial concentration at low pH, and no obvious difference was found at high pH. Scheidegger et al.[42] and Kosmulski[43] studied Ni(II) sorption on pyrophyllite and silica as a function of pH for different initial concentrations, respectively, and similar results were found. These findings interestingly suggest that the initial concentration-dependent trend of Ni(II) sorption is invariant with solid surface.

The EXAFS spectra and RSFs of sorption samples at different pH are presented in Figure 3. The amount of Ni(II) uptake increases with increasing pH, and thus pronounced oscillations are found in EXAFS signal at higher energies. The differences in the EXAFS spectra (Figure 3A) indicate that Ni(II) local atomic structure varies with pH changing. Only a single peak at ∼1.6 Å is observed in the RSF of the sample at pH 5.0 (Figure 3B), which results from O backscatter in the first shell. This indicates that the local atomic structure of adsorbed Ni(II) is similar to that of Ni(II)(aq) and an outer-sphere surface complex is formed. The result is coherent with macroscopic data, i.e., an outer-sphere surface complex is formed on diatomite surface via ion exchange.

For the samples at pH 7.0, 8.0, and 10.0, the EXAFS spectra are different from that of the sample at pH 5.0. The node at $k \approx 5.0$ Å^{-1} gradually increases in intensity with increasing pH, and the spectral feature at $k \approx 7.0-9.0$ Å^{-1} seemingly evolves with pH increasing. These two spectral modifications indicate a change of Ni coordination chemistry with pH increasing. The spectra of the two samples at pH 7.0 and 8.0 are fitted with Ni−Si1 and Ni−Si2 pairs. The spectral analysis led to the identification of two nearest shells containing 1.8 Si at $R_{Ni-Si1} \approx 3.09$ Å and 3.4 Si at $R_{Ni-Si2} \approx 3.28$ Å for the sample at pH 7.0, and 1.9 Si at $R_{Ni-Si1} \approx 3.10$ Å and 3.6 Si at $R_{Ni-Si2} \approx 3.27$ Å for the sample at pH 8.0. It has been generally regarded that mineral

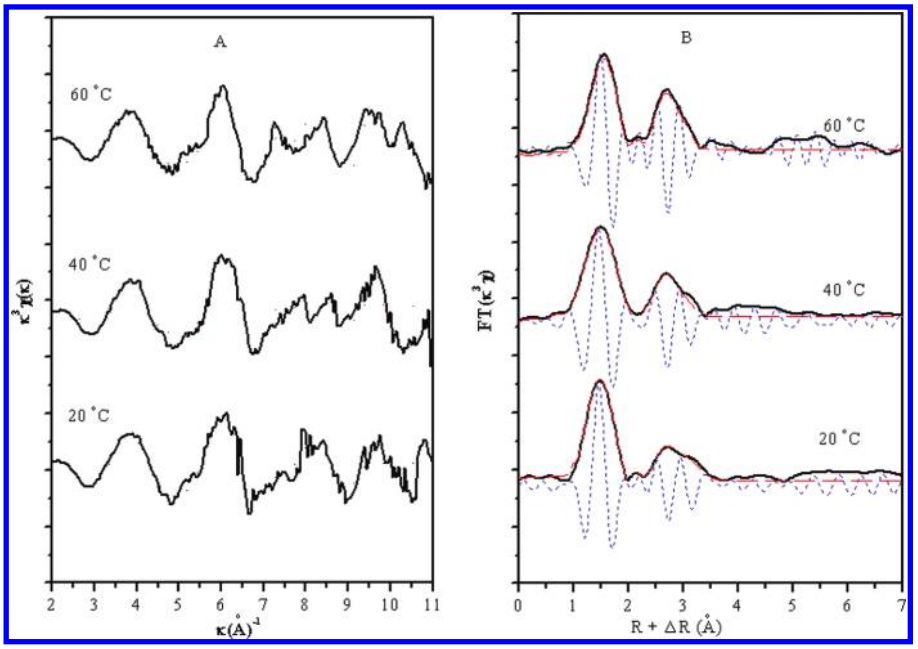

Figure 4. EXAFS spectra (A) and corresponding RSF magnitudes (solid and dashed lines represent experimental spectra and spectral fits, respectively) and imaginary parts (B) of sorption samples at various temperatures, $C_{Ni(II)initial}$ = 10 mg/L, pH = 7.0, T = 20, 40, and 60 °C, I = 0.01 M $NaNO_3$.

surface can catalyze surface (co)precipitation even metal ions can not (co)precipitate under that condition in solution, and thus surface (co)precipitates can be observed at metal surface loadings far below theoretical monolayer coverage and in a pH range well below the pH where the formation of metal hydroxide (co)-precipitates would be expected according to the thermodynamic solubility product.[38,44,45] On the basis of the above analysis, despite the low concentration of Ni(II) used in this study, Ni−Si surface coprecipitation actually occurred on diatomite surface at pH 7.0 or 8.0. The pH dependence of released Si in diatomite-water system is also conducted and the results are shown in Figure SI-4B. It is obvious that a small amount of Si was observed at pH < 9.0. Therefore, the formation of surface coprecipitates somewhat contributes to Ni sorption under the weak alkaline conditions. However, it is worth pointing out that inner-sphere complexation may occur at the surface Si−OH sites concurrently with surface coprecipitation. This finding highlights the necessity of using EXAFS to distinguish surface coprecipitates from inner-sphere complexes under weak alkaline conditions. In two comparable EXAFS studies on Ni uptake onto montmorillonite under weak alkaline conditions at high or low Ni concentration,[29,35] the formation of a neoformed Ni-phyllosilicate was observed at high Ni concentration,[35] while inner-sphere complexes were found at low Ni concentration.[29] The formation of surface (co)precipitates was found in various previous studies at elevated Ni concentration.[14−18,22−28,35] On the contrary, we have found spectroscopic evidence for the simultaneous formation of surface coprecipitates and inner-sphere complexes on diatomite surface at low Ni concentration, which is inconsistent with the results reported by Dähn et al.[29] wherein inner-sphere complexation dominates Ni sorption on montmorillonite at low Ni concentration. This finding indicates that the mechanism of Ni sorption at low concentration is mineral surface-dependent. More importantly, this study shows that, under weak alkaline conditions, the mechanism controlling Ni uptake at low concentration is different from that at high concentration. The formation of inner-sphere complexes or (co)precipitates is dependent on the initial concentration of Ni(II) in solution.

For the sample at pH 10.0, the values of $R_{Ni-Ni} \approx 3.07$ Å and $R_{Ni-Si2} \approx 3.27$ Å (Table 1) well match those in Ni phyllosilicates, implying that the nucleation of Ni phase having a Ni phyllosilicate-like local atomic structure at pH 10.0.[28,35] It can be clearly seen from Figure SI-4B that a significant amount of Si was released at pH > 9.0, which can be characterized by the following reactions: $SiO_2(amorphous) + 2H_2O = Si(OH)_4$, $Si(OH)_4 = SiO(OH)_3^- + H^+$, $SiO(OH)_3^- = SiO_2(OH)_2^{2-} + H^+$.[37,46] The similarity of dissolution property for diatomite and silica is due to the fact that the main component of diatomite is silica (Table SI-1). Based on the discussion above, it can be concluded that Ni(II) phyllosilicate can be also formed on diatomite under high alkaline conditions. However, it should be also noted that Ni surface precipitates can not be excluded due to the similarity of EXAFS spectra in k-space for $Ni(OH)_2$ and Ni phyllosilicate with the uptake samples (Figure SI-5). The present study combines Si released experiment with EXAFS studies and interestingly highlights the possibility of a mixture, containing Ni precipitates and Ni phyllosilicate, formed on Si-containing mineral at low Ni concentration under high alkaline conditions.

Temperature Effect. The sorption isotherms of Ni(II) on diatomite at 20, 40, and 60 °C are shown in Figure 1D, and detailed analysis of sorption isotherms and thermodynamic data are described in SI. The EXAFS spectra and RSFs are presented in Figure 4. For all samples, the first peak at ~1.6 Å dominates the Fourier transforms, corresponding to the Ni−O contribution and there is no significant difference in this peak. The intensity of the peak at ~2.8 Å reflecting the second coordination sphere, increases with temperature rising, which is ascribed to the increase of Ni(II) uptake at higher temperature. As shown in Table 1, the central Ni is surrounded by 1.8 Si at $R_{Ni-Si1} \approx 3.09$ Å, 3.4 Si at $R_{Ni-Si2} \approx 3.28$ Å at T = 20 °C, and 1.8 Si at $R_{Ni-Si1} \approx$ 3.09 Å, 3.8 Si at $R_{Ni-Si2} \approx 3.27$ Å at T = 40 °C, and 1.9 Si at $R_{Ni-Si1} \approx 3.09$ Å, 4.3 Si at $R_{Ni-Si2} \approx 3.27$ Å at T = 60 °C.

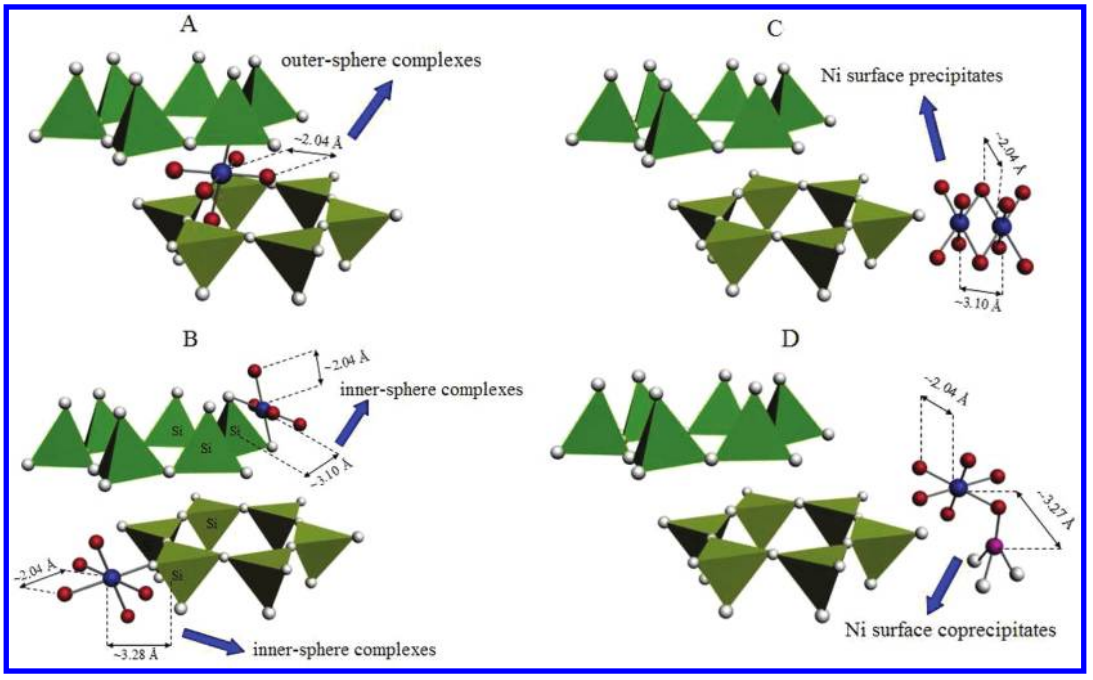

Figure 5. Mechanism illustration of Ni(II) uptake onto diatomite: A: outer-sphere complexes, B: inner-sphere complexes, C: Ni surface precipitates, D: Ni surface coprecipitates.

According to the above analysis, one can find that there is a continuum between Ni surface coprecipitates and inner-sphere sorption at diatomite surface over the three temperatures investigated. It is well-known that at low surface coverage, surface complexation dominates, while at high surface coverage, surface coprecipitates control metal uptake onto minerals.[38,44,45] Therefore, the CN values of Ni−Si2 increase obviously from ~3.4 to ~4.3 with temperature increasing from 20 to 60 °C, demonstrating that the growth of surface coprecipitates is favored at higher temperature due to the increased surface coverage (Figure 1D).

XPS Analysis. The Ni 2p XPS spectra are influenced exclusively by charge transfer process from the nearest-neighbor atoms (such as O, Ni).[47] Typical XPS spectra (Figure SI-9) show that doublets characteristic of Ni 2p at pH = 7.0 appears Ni $2p_{3/2}$ at 856.17 eV and Ni $2p_{1/2}$ at 873.82 eV, while the doublets characteristic of Ni 2p at pH = 10.0 appears Ni $2p_{3/2}$ at 856.59 eV and Ni $2p_{1/2}$ at 874.15 eV. This XPS feature is perhaps associated with inner-sphere surface complexation or surface coprecipitation at pH = 7.0 and a mixture of surface precipitation and Ni phyllosilicate at pH = 10.0. Figure SI-9 also shows the O 1s XPS spectra at ~532 eV. The O 1s peak can be deconvoluted into three components, which can be assigned to bridging OH (~531.7 eV), terminal OH (~532.6 eV), and adsorbed H_2O (~533.2 eV). There is no significant difference between the oxygen peaks at pH = 7.0 and pH = 10.0, suggesting that the environment surrounding O does not change under variation of pH.

Environmental Implication. Complementary macroscopic and microscopic experiments reported herein demonstrate that Ni(II) could be retained on diatomite via different mechanisms (Figure 5), depending on various environmental conditions such as time, pH, and temperature. At low pH (i.e., pH 5.0), the uptake of Ni(II) is via outer-sphere complexation in the interlayer space where the ion exchange site (XNa/H) might be located (Figure 5A). At pH 7.0 and 8.0, Ni(II) sorption is dominated by inner-sphere surface complexation (Figure 5B) and surface coprecipitation (Figure 5D). The uptake of Ni(II) at pH 10.0 is attributed to the formation of Ni surface precipitates (Figure 5C) and/or Ni phyllosilicate-like surface coprecipitation (Figure 5D). In addition, surface (co)precipitates also dominate Ni uptake when the reaction time extended to 1 month. Furthermore, the sorption capacity increases with temperature increasing, which indicates that surface coprecipitates become the dominant mechanism at elevated temperature. The attachment of Ni(II) on diatomite surfaces can reduce their mobility in environmental media. The information presented herein will allow scientists and engineers to develop better models to evaluate Ni(II) interaction with clay minerals. This study also demonstrates the utility of the EXAFS technique to distinguish different sorption mechanisms of Ni(II) onto diatomite. The findings of this work are of great environmental importance toward a molecular-level description of Ni(II) and related transition metal ions uptake mechanism at water−mineral interface.

■ ASSOCIATED CONTENT

Supporting Information. Characterization of diatomite, sample preparation for XPS and EXAFS study and EXAFS analysis of the reference samples, batch experimental results, XPS spectra. This material is available free of charge via the Internet at http://pubs.acs.org.

■ AUTHOR INFORMATION

Corresponding Author

*Tel: +86-551-5592788; fax: +86-551-5591310; e-mail: xkwang@ipp.ac.cn.

Author Contributions

G. Sheng and S. Yang contributed equally to this paper.

■ ACKNOWLEDGMENT

Financial support from 973 projects (2011CB933700, 2007CB936602), NSFC (20907055, 20971126), and open foundation of State Key Lab of Pollution Control and Resource Reuse are acknowledged. We gratefully acknowledge Dr. Fengchun Hu and Dr. Zhi Xie of NSRL, USTC for helpful technical assistance of EXAFS experiments. Thanks are also extended to Prof. D. A. Dzombak and the anonymous reviewers for their helpful comments to improve the quality of our manuscript.

■ REFERENCES

(1) Nriagu, J. O.; Pacyna, J. M. Quantitative assessment of worldwide contamination of air, water and soils by trace metals. *Nature* **1988**, *333*, 134–139.

(2) Trivedi, P.; Axe, L.; Tyson, T. XAS studies of Ni and Zn sorbed to hydrous manganese oxide. *Environ. Sci. Technol.* **2001**, *35*, 4515–4521.

(3) Marcussen, H.; Holm, P. E.; Strobel, B. W.; Hansen, H. C. B. Nickel sorption to goethite and montmorillonite in presence of citrate. *Environ. Sci. Technol.* **2009**, *43*, 1122–1127.

(4) Osmanlioglu, A. E. Natural diatomite process for removal of radioactivity from liquid waste. *Appl. Radiat. Isot.* **2007**, *65*, 17–20.

(5) Gürü, M.; Venedik, D.; Murathan, A. Removal of trivalent chromium from water using low-cost natural diatomite. *J. Hazard. Mater.* **2008**, *160*, 318–323.

(6) Khraisheh, M. A. M.; Al-degs, Y. S.; Mcminn, W. A. M. Remediation of wastewater containing heavy metals using raw and modified diatomite. *Chem. Eng. J.* **2004**, *99*, 177–184.

(7) Al-Degs, Y.; Khraisheh, M. A. M.; Tutunji, M. F. Sorption of lead ions on diatomite and manganese oxides modified diatomite. *Water Res.* **2001**, *15*, 3724–3728.

(8) Sheng, G. D.; Hu, J.; Wang, X. K. Sorption properties of Th(IV) on the raw diatomite-Effects of contact time, pH, ionic strength and temperature. *Appl. Radiat. Isot.* **2008**, *66*, 1313–1320.

(9) Sheng, G. D.; Wang, S. W.; Hu, J.; Lu, Y.; Li, J. X.; Dong, Y. H.; Wang, X. K. Adsorption of Pb(II) on diatomite as affected via aqueous solution chemistry and temperature. *Colloids Surf., A* **2009**, *339*, 159–166.

(10) Strathmann, T. J.; Myneni, S. B. Effect of soil fulvic acid on Nickel(II) sorption and bonding at the aqueous-boehmite (γ-AlOOH) interface. *Environ. Sci. Technol.* **2005**, *39*, 4027–4034.

(11) Takamatsu, R.; Asakura, K.; Chun, W.; Miyazaki, T.; Nakano, M. EXAFS studies about the sorption of cadmium ions on montmorillonite. *Chem. Lett.* **2006**, *35*, 224–225.

(12) Vasconcelos, I. F.; Haack, E. A.; Maurice, P. A.; Bunker, B. A. EXAFS analysis of cadmium(II) adsorption to kaolinite. *Chem. Geol.* **2008**, *249*, 237–249.

(13) Stumpf, Th.; Hennig, C.; Bauer, A.; Denecke, M. A.; Fanghänel, Th. An EXAFS and TRLFS study of the sorption of trivalent actinides onto smectite and kaolinite. *Radiochim. Acta* **2004**, *92*, 133–138.

(14) Roberts, D. R.; Scheidegger, A. M.; Sparks, D. L. Kinetics of mixed Ni-Al precipitate formation on a soil clay fraction. *Environ. Sci. Technol.* **1999**, *33*, 3749–3754.

(15) Nachtegaal, M.; Sparks, D. L. Nickel sequestration in a kaolinite-humic acid complex. *Environ. Sci. Technol.* **2003**, *37*, 529–534.

(16) Ford, R. G.; Scheckel, K. G.; Sparks, D. L.; Scheinost, A. C. The link between clay mineral weathering and the stabilization of Ni surface precipitates. *Environ. Sci. Technol.* **1999**, *33*, 3140–3144.

(17) Scheidegger, A. M.; Lamble, G. M.; Sparks, D. L. Spectroscopic evidence for the formation of mixed-cation hydroxide phases upon metal sorption on clays and aluminum oxides. *J. Colloid Interface Sci.* **1997**, *186*, 118–128.

(18) Scheinost, A. C.; Sparks, D. L. Formation of layered single- and double-metal hydroxide precipitates at the mineral/water interface: A multiple-scattering XAFS analysis. *J. Colloid Interface Sci.* **2000**, *223*, 167–178.

(19) Fandeur, D.; Juillot, F.; Morin, G.; Olivi, L.; Cognigni, A.; Webb, S. M.; Ambrosi, J. P.; Fritsch, E.; Guyot, F.; Brown, G. E., Jr. XANES evidence for oxidation of Cr(III) to Cr(VI) by Mn-oxides in a lateritic regolith developed on serpentinized ultramafic rocks of new-caledonia. *Environ. Sci. Technol.* **2009**, *43*, 7384–7390.

(20) Landrot, G.; Ginder-Vogel, M.; Sparks, D. L. Kinetics of chromium(III) oxidation by manganese(IV) oxides using quick scanning X-ray absorption fine structure spectroscopy (Q-XAFS). *Environ. Sci. Technol.* **2010**, *44*, 143–149.

(21) Vespa, M.; Dähn, R.; Gallucci, E.; Grolimund, D.; Wieland, E.; Scheidegger, A. M. Microscale investigations of Ni uptake by cement using a combination of scanning electron microscopy and synchrotron-based techniques. *Environ. Sci. Technol.* **2006**, *40*, 7702–7709.

(22) Elzinga, E. J.; Sparks, D. L. Reaction condition effects on Nickel sorption mechanisms in illite-water suspensions. *Soil Sci. Soc. Am. J.* **2001**, *65*, 94–101.

(23) Elzinga, E. J.; Sparks, D. L. Nickel sorption mechanisms in a pyrophyllite montmorillonite mixture. *J. Colloid Interface Sci.* **1999**, *213*, 506–512.

(24) Livi, K. J. T.; Senesi, G. S.; Scheinost, A. C.; Sparks, D. L. Microscopic examination of nanosized mixed Ni-Al hydroxide surface precipitates on pyrophyllite. *Environ. Sci. Technol.* **2009**, *43*, 1299–1304.

(25) Paulhiac, J. L.; Clause, O. Surface coprecipitation of cobalt(II), nickel(II), or zinc(II) with aluminum(III) ions during impregnation of gamma-alumina at neutral pH. *J. Am. Chem. Soc.* **1993**, *115*, 11602–11603.

(26) d'Espinose de la Caillerie, J. B.; Kermarec, M.; Clause, O. Impregnation of γ-alumina with Ni(II) and Co(II) ions at neutral pH: Hydrotalcite-type coprecipitate formation and characterization. *J. Am. Chem. Soc.* **1995**, *117*, 11471–11481.

(27) Scheinost, A. C.; Ford, R. G.; Sparks, D. L. The role of Al in the formation of secondary Ni precipitates on pyrophyllite, gibbsite, talc, and amorphous silica: A DRS study. *Geochim. Cosmochim. Acta* **1999**, *63*, 3193–3203.

(28) Charlet, L.; Manceau, A. Evidence for the neoformation of clays upon sorption of Co(II) and Ni(II) on silicates. *Geochim. Cosmochim. Acta* **1994**, *58*, 2577–2582.

(29) Dähn, R.; Scheidegger, A. M.; Manceau, A.; Schlegel, M. L.; Baeyens, B.; Bradbury, M. H.; Chateigner, D. Structural evidence for the sorption of Ni(II) atoms on the edges of montmorillonite clay minerals: A polarized X-ray absorption fine structure study. *Geochim. Cosmochim. Acta* **2003**, *67*, 1–15.

(30) Li, W.; Pan, G.; Zhang, M.; Zhao, D.; Yang, Y.; Chen, H.; He, G. EXAFS studies on adsorption irreversibility of Zn(II) on TiO_2: Temperature dependence. *J. Colloid Interface Sci.* **2008**, *319*, 385–391.

(31) Catalano, J. G.; Warner, J. A.; Brown, G. E., Jr. Sorption and precipitation of Co(II) in Hanford sediments and alkaline aluminate solutions. *Appl. Geochem.* **2005**, *20*, 193–205.

(32) Lee, S.; Anderson, P. R.; Bunker, G. B.; Karanfil, C. EXAFS study of Zn sorption mechanisms on montmorillonite. *Environ. Sci. Technol.* **2004**, *38*, 5426–5432.

(33) Xu, Y.; Axe, L.; Boonfueng, T.; Tyson, T. A.; Trivedi, P. Ni(II) complexation to amorphous hydrous ferric oxide: An X-ray absorption spectroscopy study. *J. Colloid Interface Sci.* **2007**, *314*, 10–17.

(34) Spadini, L.; Manceau, A.; Schindler, P. W.; Charlet, L. Structure and stability of Cd^{2+} surface complexes on ferric oxides. I. Results from EXAFS spectroscopy. *J. Colloid Interface Sci.* **1994**, *168*, 73–86.

(35) Dähn, R.; Scheidegger, A. M.; Manceau, A.; Schlegel, M. L.; Baeyens, B.; Bradbury, M. H.; Morales, M. Neoformation of Ni phyllosilicate upon Ni uptake on montmorillonite: A kinetics study by powder and polarized extended X-ray absorption fine structure spectroscopy. *Geochim. Cosmochim. Acta* **2002**, *66*, 2335–2347.

(36) Schlegel, M. L.; Manceau, A.; Charlet, L.; Chateigner, D. L.; Hazemann, J. L. Sorption of metal ions on clay minerals. III. Nucleation and epitaxial growth of Zn phyllosilicate on the edges of hectorite. *Geochim. Cosmochim. Acta* **2001**, *65*, 4155–4170.

(37) Takahashi, Y.; Murata, M.; Kimura, T. Interaction of Eu(III) ion and non-porous silica: Irreversible sorption of Eu(III) on silica and

hydrolysis of silica promoted by Eu(III). *J. Alloys Compd.* **2006**, *408*−*412*, 1246–1251.

(38) Scheidegger, A. M.; Strawn, D. G.; Lamble, G. M.; Sparks, D. L. The kinetics of mixed Ni-Al hydroxide formation on clay and aluminum oxide minerals: A time-resolved XAFS study. *Geochim. Cosmochim. Acta* **1998**, *62*, 2233–2245.

(39) Hayes, K. F.; Leckie, J. O. Modeling ionic strength effects on cation adsorption at hydrous oxide/solution interfaces. *J. Colloid Interface Sci.* **1987**, *115*, 564–572.

(40) Pathak, P. N.; Choppin, G. R. Nickel(II) sorption on hydrous silica: A kinetic and thermodynamic study. *J. Radioanal. Nucl. Chem.* **2006**, *268*, 467–473.

(41) Saeki, K.; Kunito, T. Estimating sorption affinities of heavy metals on humic acid and silica using a constant capacitance model. *Commun. Soil Sci. Plant Anal.* **2009**, *40*, 3252–3262.

(42) Scheidegger, A. M.; Fendorf, M.; Sparks, D. L. Mechanisms of Nickel sorption on pyrophyllite: Macroscopic and microscopic approaches. *Soil Sci. Soc. Am. J.* **1996**, *60*, 1763–1772.

(43) Kosmulski, M. The effect of the ionic strength on the adsorption isotherms of nickel on silica. *J. Colloid Interface Sci.* **1997**, *190*, 212–223.

(44) Scheidegger, A. M.; Lamble, G. M.; Sparks, D. L. Investigation of Ni Sorption on Pyrophyllite: An XAFS Study. *Environ. Sci. Technol.* **1996**, *30*, 548–554.

(45) Scheckel, K. G.; Sparks, D. L. Kinetics of the formation and dissolution of Ni precipitates in a gibbsite/amorphous silica mixture. *J. Colloid Interface Sci.* **2000**, *229*, 222–229.

(46) Kar, A. S.; Tomar, B. S.; Godbole, S. V.; Manchanda, V. K. Time resolved fluorescence spectroscopy and modeling of Eu(III) sorption by silica in presence and absence of alpha hydroxy isobutyric acid. *Colloids Surf., A* **2011**, *378*, 44–49.

(47) Hattori, Y.; Konishi, T.; Kaneko, K. XAFS and XPS studies on the enhancement of methane adsorption by NiO dispersed ACF with the relevance to structural change of NiO. *Chem. Phys. Lett.* **2002**, *355*, 37–42.